ELECTRICITY PRICE DEPENDENCE IN NEW YORK STATE ZONES: A ROBUST DETRENDED CORRELATION APPROACH[1]

BY DEBBIE J. DUPUIS

HEC Montréal

The cost of electricity varies across the zones of the New York State electric system. While fair and open access to the electrical grid is sought, we show that residents currently do not equally benefit, or suffer, from price changes. Upcoming major investments in the grid offer an opportunity to rectify these inequalities, but only if we understand the price-change propagation dynamics for the current underlying infrastructure. We study these dynamics, estimating the partial correlations between changes in electricity prices in connected zones. We develop and investigate a robust exponentially weighted correlation estimator that performs well in the presence of electricity price spikes and can track a rapidly changing time-varying correlation. We show that price-change partial correlations are mostly positive, but can also be negative, and provide new insight into price-change dynamics within the grid that cannot be extracted from the price-setting algorithm or obtained from available transmission capability data.

1. Introduction. After many decades of electricity markets dominated by regulated monopolies, there was a movement to restructure the electricity industry in the 1990s. Driven by the desire to address high electricity prices, some U.S. states opted to deregulate the electric utility industry. The New York Independent System Operator (NYISO) was created in 1999 to facilitate the restructuring of the industry in the state of New York. The NYISO's mission is to provide fair and open access to the electrical grid, maintain and enhance regional reliability, provide factual information to policymakers, stakeholders and investors in the power system, and plan the power system for the future.[2] In a deregulated electricity market, load serving entities (or distributors) provide bids to purchase energy and power suppliers (or generators) provide offers to sell energy. The NYISO manages these market transactions and schedules energy sales and purchases in multiple locations across the state.

Locational Based Marginal Pricing (LBMP) is a pricing methodology for the cost of energy at each location in the New York State transmission system. LBMP is essentially the cost to serve the next megawatt (MW) of load at a specific lo-

[2]The NYISO Mission, www.nyiso.com.

cation on the grid, and it is determined by the NYISO following bids and offers. Congestion and transmission losses lead to unequal LBMP at different locations.[3] Referring to the heat wave of July 2013, the New York Independent System Operator (2014) states "Periods of resource scarcity during the heat wave produced price spikes and illustrated the challenges of serving historically-congested areas of the Lower Hudson Valley, New York City and Long Island. Demand response was targeted to those regions at the start of the heat wave. In the future, transmission upgrades into and/or development of generation and demand-side resources in those areas would alleviate congestion, help avoid future reliability problems, lower consumers' energy costs, and enhance operational flexibility." The New York Independent System Operator (2014)[4] also states that "More than 80 percent of New York's high-voltage transmission lines went into service before 1980. Of the state's more than 11,000 circuit-miles of transmission lines, nearly 4700 circuit-miles will require replacement within the next 30 years, at an estimated cost of $25 billion."

Any replacement and/or upgrade should minimally improve market efficiency and serve more equitably all residents of the state. Determining the extent to which changes in electricity price coincide across different locations is made particularly difficult by the presence of electricity price spikes. Electricity price spikes do not only occur during heat waves, but are actually quite frequent [see, e.g., Eydeland and Wolyniec (2012)]. Unexpected increases in demand, unexpected shortfalls in supply and failure of the transmission infrastructure can cause electricity prices to suddenly jump to very high levels [Geman and Roncorni (2006)]. We are not interested in electricity price forecasting; see, for example, Hickey, Loomis and Mohammadi (2012) and Nowotarski, Tomczyk and Weron (2013). Our goal is also not to identify spikes [see Janczura et al. (2013)], forecast spikes [see Christensen, Hurn and Lindsay (2012)] or explain spikes [see Hellström, Lundgren and Yu (2012)]. Rather, we wish to estimate the correlations between changes in electricity prices at different locations in the presence of these spikes. More robust estimators than the usual Pearson correlation exist, for example, Spearman's rho or Kendall's tau. The time-varying nature of the correlations must be considered however. We calculate Spearman's rho over moving windows, apply a recently developed [Pozzi, Di Matteo and Aste (2012)] exponentially weighted Kendall's tau and develop another well-suited and better performing robust alternative.

Our main contributions are twofold. First, we develop and investigate a robust exponentially weighted correlation estimator that performs well in the presence of spikes and can track a rapidly changing time-varying correlation. Second, we provide an assessment of the current level of dependence between price changes in connected zones. The sophistication of the price-setting algorithm [see New York Independent System Operator (2013)] and the electrical grid do not allow for an

---

[3]The state of New York is divided into 11 zones. These are explained in Section 2.

[4]Citing New York's State Transmission Assessment and Reliability Study Phase II Study Report, STARS Technical Working Group, March 30, 2012.
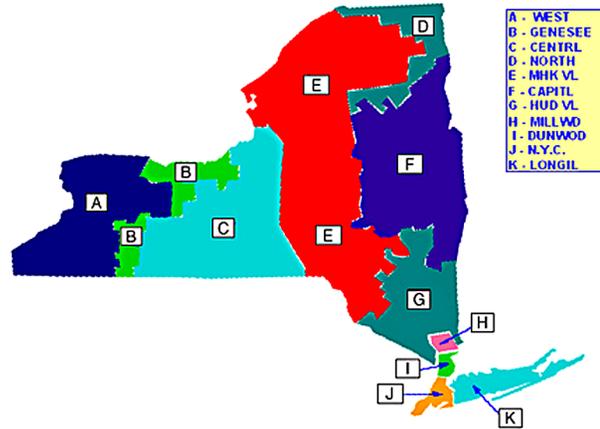
FIG. 1.   *New York Control Area internal zones*. *Source*: *NYISO*.

ex ante analysis of the dependencies. Our ex-post analysis is the first to reveal the dependencies resulting from the current protocols, practices and infrastructure. We also assess how these dependencies are affected by contemporaneous variables like temperature, time of day, price of natural gas, etc. Our correlation estimates and innovative subsequent exploratory data analysis provide new insight that can assist planners in determining the nature of transmission upgrades, or the location and capacity of generation development and demand-side resources, that could improve the electricity market.

The remainder of the paper is organized as follows. In Section 2, we present the electricity price data and discuss marginal models. In Section 3, we review correlation estimators and present our robust exponentially weighted midcorrelation estimator. Its properties are investigated in Section 4 through a simulation study. The electricity price data are analyzed in Section 5 and a discussion appears in Section 6.

2. New York State electricity prices by zone.   We consider the Day Ahead Market Zonal LBMP electricity price in \$/MWHr for each zone in the state of New York over the 1 January 2009 to 31 December 2014 period. Data are hourly prices and are available from NYISO at www.nyiso.com. There are 15 New York Control Area (NYCA) zones: 11 internal[5] and 4 external.[6] The 11 internal NYCA zones are shown in Figure 1. The external zone PJM connects at zones A, C, G and J; Hydro-Quebec connects at zone D; NPX connects at zones D, F and K; and Ontario Hydro connects at zones A and D. Data are plotted in Figure 2.

---

[5]A—West; B—Genesee; C—Central; D—North; E—Mohawk Valley; F—Capital; G—Hudson Valley; H—Millwood; I—Dunwoodie; J—New York City; K—Long Island.

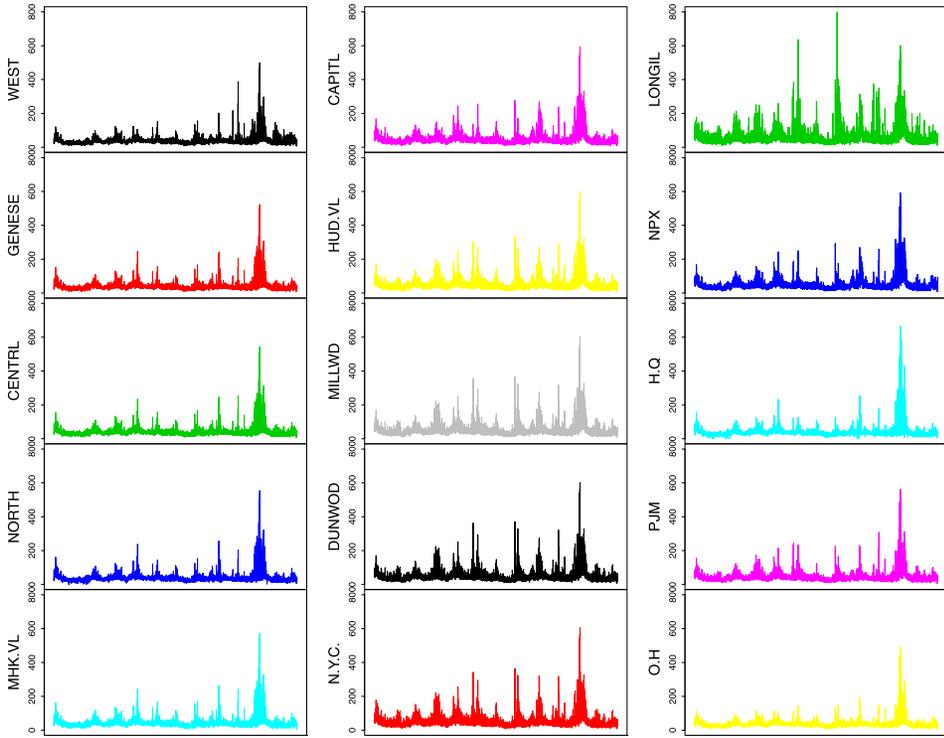[6]PJM, Hydro Quebec, NPX and Ontario Hydro.

FIG. 2. *Hourly Day Ahead Market Zonal Locational Based Marginal Pricing* (*LBMP*) *electricity price in $/MWHr for each zone in the state of New York over the* 1 *January* 2009 *to* 31 *December* 2014 *period.*

The presence of cyclical and seasonal patterns in prices is well documented. See Hickey, Loomis and Mohammadi (2012) for a recent review of the problem and possible modeling approaches. Following the standard practice with asset prices, we consider log returns of the LBMP hourly price to obtain more stationary series; see Figure 3. Returns also show cyclical and seasonal patterns. The presence of spikes in the electricity price is also well documented [see, e.g., Eydeland and Wolyniec (2012)]. These spikes yield outliers in the returns and warrant the use of robust estimation methods to deseasonalize. When the mean model is robustly estimated, the distribution of residuals are heavy tailed, and the residuals show autocorrelation and seasonal autocorrelation. When recent lags and seasonal lags are included in the model to eliminate this dependence in the residuals, unaccounted for differences also show cyclical and seasonal patterns in their variability, as well as volatility clustering, and retain the spikes of the series. To avoid unnecessarily large and persistent volatility following spikes and to produce more robust fits, we use log-GARCH models [Sucarrat, Grønneberg and Escribano (2016)] since they provide greater robustness to jumps and outliers. These models are attractive as they guarantee the positivity of volatility without constraining the parameters. The
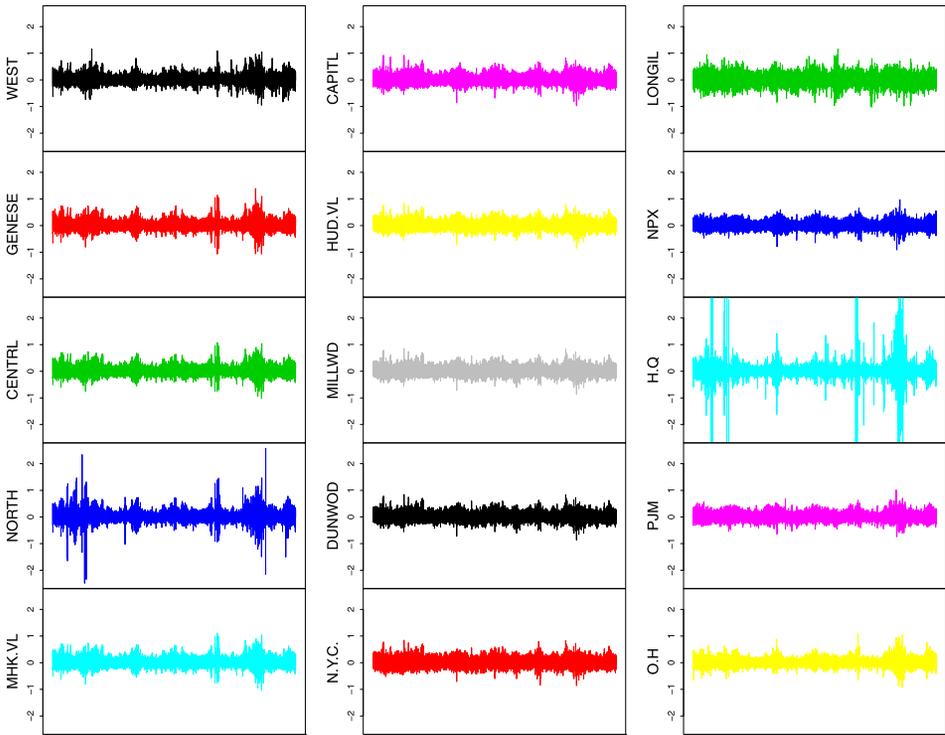
FIG. 3. *Hourly returns on Day Ahead Market Zonal Locational Based Marginal Pricing* (*LBMP*) *electricity price in $/MWHr for each zone in the state of New York over the* 1 *January* 2009 *to* 31 *December* 2014 *period.*

log-GARCH-X class easily includes explanatory variables to model any cyclical or seasonal patterns in the volatility. Additionally, as the dynamics of the returns in different zones can be strongly related (see, e.g., Figure 3), these series may exhibit volatility spillovers. We proceed as in Francq and Sucarrat (2017) where other return series are included as explanatory variables for the volatility of a given series to capture any spillovers.[7] The volatility equation for a given return series can also include the lagged sign of the return as an explanatory variable to produce an asymmetric log-GARCH model. We take this approach here; see Francq and Sucarrat (2017) for more details. The main drawback of the log-GARCH model is that the returns have to be nonnull. This was not an issue here, as while there are zero log-returns in the data, the log-returns are deseasonalized/demeaned prior to the fitting of the log-GARCH model and none of the residuals are equal to zero. Solutions to the nonnull returns issue do exist; see Sucarrat and Escribano (2014).

---

[7]The resulting univariate volatility equation is consistent with the marginal in the multivariate log-GARCH-X specification, however, we do not pursue the full multivariate specification here.

2.1. *Mean and variance models.* In electricity markets, variation of demand, costs and constraints lead to distinct price profiles for each hourly trading period. Authors in the price forecasting literature [see, e.g., Karakatsani and Bunn (2008), Pẽna (2012) and the references therein] estimate price models separately for each period in order to control for these dissimilarities. We proceed analogously with our hourly log returns. More precisely, let $Y_{h(t)}$ be the log return $[Y_{h(t)} = \Delta \ln L_{h(t)}$, where $L_{h(t)}$ is the LBMP electricity price in \$/MWHr] at hour h in day t. We consider the time series model

$$(1) \qquad \Phi(B^S)\phi(B)(Y_{h(t)} - \mu_{h(t)}) = \varepsilon_{h(t)},$$

$$(2) \qquad \varepsilon_{h(t)} = \sigma_{h(t)} z_{h(t)},$$

where

$$(3) \qquad \mu_{h(t)} = \omega + \boldsymbol{\gamma}' \boldsymbol{D}_{h(t)} + \boldsymbol{\xi}' \boldsymbol{X}_{h(t)},$$

$$(4) \qquad \ln \sigma_{h(t)}^2 = \alpha_0 + \alpha_1 \ln \varepsilon_{h(t-1)}^2 + \beta_1 \ln \sigma_{h(t-1)}^2 + \boldsymbol{\lambda}' \boldsymbol{D}_{h(t)} + \boldsymbol{\zeta}' \boldsymbol{X}_{h(t)},$$

and B denotes the backshift operator, $\phi(B)$ is an autoregressive polynomial of order p, $\Phi(B)$ is a seasonal autoregressive polynomial of order P, $S = 7$ to capture the stochastic weekly patterns, $\boldsymbol{D}_{h(t)}$ is a matrix of dummy variables for deterministic components (day of the week, holidays), $\boldsymbol{X}_{h(t)}$ is a matrix of contemporaneous time-varying variables, and $z_{h(t)} \sim$ stationary. Explanatory variables need not be exogenous nor independent of the standardized error. We include a leverage term $I_{\varepsilon_{h(t-1)} < 0}$ and volatility proxies for other zones, say, $\ln(\varepsilon_{-i,h(t-1)}^2)$, where $-i$ means without zone i in a model for zone i, to allow for volatility spillovers; see Francq and Sucarrat (2017) for details.

2.2. *Estimation.* Estimates for the parameters in (1)–(4) are obtained in three steps. First, the mean model in (3) is fitted robustly using the method of the least median of squares. The residuals, that is, detrended log returns, from the estimated mean model (3) are then used for the estimation of the parameters $\phi_1, \ldots, \phi_p$ and $\Phi_1, \ldots, \Phi_P$ in (1). These parameters are also estimated robustly using the method of the least median of squares. The residuals from this second robust regression are then used for the estimation of the parameters in the log-volatility specification. The log-GARCH(1, 1) model with external regressors in (4) is estimated using the lgarch package in R [Sucarrat (2014)]. A weighted Portmanteau test is carried out to check that the series are well devolatilized by our log-GARCH-X models. We use the weighted version of the statistic proposed by Li and Mak (1994) implemented in the WeightedPortTest package in R [Fisher and Gallagher (2012)]. We wish to assess the correlation between the residuals of model (4), which are the detrended-devolatilized log returns, from each of the NYCA zones.

3. Correlation. A simple statistical measure of co-movements between two random variables is covariance. Given observations (x_i, y_i), $i = 1, \ldots, n$ of two random variables X and Y, the sample covariance is defined as

$$c_{xy} = \frac{1}{n-1} \sum_{i=1}^{n} (x_i - \bar{x})(y_i - \bar{y}).$$

The sample Pearson correlation coefficient is defined as

$$r = \frac{c_{xy}}{\sqrt{c_{xx}c_{yy}}}.$$

Historical returns are used to estimate the covariances, and correlations, among present returns. When all returns, past and present, are drawn from a stable joint distribution, it is desirable to use as many past observations as possible in order to maximize the accuracy of the resulting estimates of the true underlying process that describes the present. However, when parameters of the distribution are changing over time, the situation is more difficult. Large amounts of past data are possibly irrelevant, and a focus on the recent past is likely to be more appropriate, but substantial estimation errors could result.

3.1. *Exponentially weighted correlation.* An exponential weighting scheme assigns a weight to an observation that is the multiple of the weight assigned to its predecessor; that is, more weight is assigned to the recent past than the distant past.

More precisely, for some $\lambda \in (0, 1)$, the exponentially weighted moving average is defined as

$$e(x) = \sum_{i=1}^{n} \frac{(1-\lambda)\lambda^{n-i}}{1-\lambda^n} x_i.$$

Note that $\sum_{i=1}^{n} (1-\lambda)\lambda^{n-i}/(1-\lambda^n) = 1$; the nth observation gets the largest weight, $(1-\lambda)/(1-\lambda^n)$, the $(n-1)$th observation gets the second largest weight, $(1-\lambda)\lambda/(1-\lambda^n)$, etc...., with each observation only getting a λ fraction of the weight of the observation that followed it.

The exponentially weighted moving covariance is most generally defined as

$$e_{xy} = \sum_{i=1}^{n} \frac{(1-\lambda)\lambda^{n-i}}{1-\lambda^n} (x_i - e(x))(y_i - e(y)),$$

although it is also common not to center the returns when using e_{xx} and e_{xy} for volatility forecasting; see, for example, Alexander (2001).

The exponentially weighted moving correlation is thus defined as

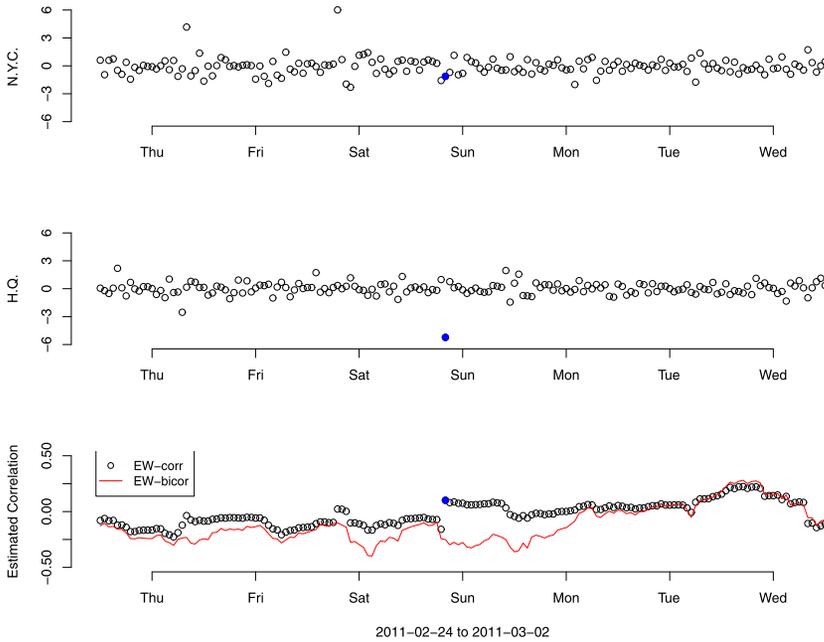$$(5) \qquad\qquad r_e = \frac{e_{xy}}{\sqrt{e_{xx}e_{yy}}}.$$

FIG. 4.   *Impact of electricity price spikes on estimated correlation. Detrended-devolatilized hourly log returns for zones N.Y.C. and H.Q. are shown in the top and middle panels, respectively. The bottom panel shows estimated correlation. Data are for week of* 2011-02-24 *to* 2011-03-02. *Values for* 11*am on* 2011-02-27 *appear as solid circles.*

In the case of LBMP electricity prices in the state of New York, detrended-devolatilized log returns can have very long tails, and the usual Pearson-like exponentially weighted moving correlation in (5) yields misleading results. This is highlighted in Figure 4 where nonrobust and robust (to be introduced in Section 3.4) estimates of the correlation are shown for the week of 24 February 2011 to 2 March 2011 for zones N.Y.C. and H.Q. The electricity price downward spike (the price dropped 17%; accounting for trend, season and volatility, this is large) at 11am on 27 February 2011 in zone H.Q. makes the nonrobust estimate of correlation breakdown. Nonrobust Pearson-like correlation estimates for that hour, and roughly the next 36 hours, are not representative of the level of dependence.

3.2. *Spearman's rho and Kendall's tau.*   It is well known that the Pearson correlation is susceptible to outliers. Several more robust measures of dependence have been proposed, for example, Spearman's rho or Kendall's tau. The Spearman correlation coefficient r_s is defined as the Pearson correlation coefficient between the ranked variables, that is,

$$(6) \qquad r_s = \frac{c_{R(x)R(y)}}{\sqrt{c_{R(x)R(x)}c_{R(y)R(y)}}},$$

where $R(\cdot)$ is used to denote ranks. Spearman's rho is, however, not amenable to exponential weighting.

Kendall's tau measures dependence differently, providing an estimate for the probability of concordance minus the probability of discordance. The sample Kendall's tau is defined as

$$\tau = \frac{2}{n(n-1)} \sum_{i=1}^{n-1} \sum_{j=i+1}^{n} \text{sgn}(x_i - x_j)\,\text{sgn}(y_i - y_j),$$

where sgn is the sign function. Pozzi, Di Matteo and Aste (2012) developed an exponential weighting Kendall's tau following

$$(7) \qquad\qquad \tau_e = \sum_{i=1}^{n-1} \sum_{j=i+1}^{n} w_{ij}\,\text{sgn}(x_i - x_j)\,\text{sgn}(y_i - y_j),$$

where $w_{ij} = w_0 \exp[\alpha(i + j - 2n)]$ and

$$w_0(\alpha) = \frac{[\exp(\alpha) - 1]^2[\exp(\alpha) + 1]}{\exp(2\alpha)[1 - \exp(-\alpha n)][1 - \exp(-\alpha(n-1))]}.$$

The proximity of observations (x_i, y_i) and (x_j, y_j) to (x_n, y_n) is considered to attribute the weight, and the exponential decay factor is $\alpha \geq 0$. The largest weight is for the $i = n - 1$, $j = n$ case.

3.3. Biweight midcorrelation.

Let X have distribution function F, let $T(F)$ and $\eta(F)$ be location and scale functionals, respectively, and let Ψ be an odd function having a first derivative. Shoemaker and Hettmansperger (1982) define the midvariance as

$$\gamma^2(F) = K^2 \eta^2 \mathrm{E}_F\{\Psi^2(U)\}/[\mathrm{E}_F\{\Psi'(U)\}]^2,$$

where $U = \{X - T(F)\}/\{K\eta(F)\}$ and K is a specified constant. The midvariance arises naturally as the asymptotic variance of M-estimates of location. It is shown that the midvariance responds to heavy tails, but is not drastically affected, and has a bounded influence curve and positive breakdown point [Shoemaker and Hettmansperger (1982)]. An estimator of the midvariance is easily found by considering the empirical distribution function.

Following the same reasoning, Wilcox (2012) defines a measure of covariance between X and Y as

$$n K^2 \eta_x \eta_y \mathrm{E}_F\{\Psi(U)\Psi(V)\}/[\mathrm{E}_F\{\Psi'(U)\Psi'(V)\}],$$

where now F is the distribution function of (X, Y). Setting $K = 9$, T to be the functional of the median, η to be the functional of the median absolute deviation,

and $\Psi(x)$ equal to the biweight function $x(1 - x^2)^2$ for $|x| < 1$ and 0 otherwise, we consider the biweight midcovariance of Wilcox (2012):

$$s_{bxy} = \frac{n \sum_{i=1}^{n} a_i (x_i - \mathrm{med}(x))(1 - u_i^2) b_i (y_i - \mathrm{med}(y))(1 - v_i^2)}{[\sum_{i=1}^{n} a_i (1 - 5u_i^2)][\sum_{i=1}^{n} b_i (1 - 5v_i^2)]},$$

where the weights a_i and b_i are defined following

$$a_i = (1 - u_i^2) I(1 - |u_i|) \quad \text{and} \quad b_i = (1 - v_i^2) I(1 - |v_i|),$$

where $I(z)$ equals 1 if $z \geq 0$ and 0 otherwise, and

$$u_i = \frac{x_i - \mathrm{med}(x)}{9 \, \mathrm{mad}(x)} \quad \text{and} \quad v_i = \frac{y_i - \mathrm{med}(y)}{9 \, \mathrm{mad}(y)}.$$

The notation med denotes the median and mad denotes the raw median absolute deviation, that is, the median of the absolute deviations from the median without the adjustment factor for asymptotically normal consistency. The biweight mid-correlation is then defined as

$$(8) \qquad r_b = \frac{s_{bxy}}{\sqrt{s_{bxx} s_{byy}}}.$$

A biweight midvariance s_{bxx} using the weight function a_i gave the best estimates of scale for several symmetric long-tailed distributions in the study of Lax (1985). The robust biweight midcorrelation can also be effectively used to suppress the effects of outliers when defining a network; see Langfelder and Horvath (2008) and Langfelder and Horvath (2012).

3.4. *Robust exponentially weighted midcorrelation.* Letting $w_i = (1 - \lambda)\lambda^{n-i}/(1 - \lambda^n)$, $i = 1, \ldots, n$, we define the exponentially weighted biweight midcovariance as

$$s_{wbxy} = \left(n \sum_{i=1}^{n} w_i a_i^w (x_i - \mathrm{wmed}(x, w))(1 - u_i^w u_i^w) \right.$$

$$\times \left. b_i^w (y_i - \mathrm{wmed}(y, w))(1 - v_i^w v_i^w) \right)$$

$$\Big/ \left(\left[\sum_{i=1}^{n} w_i a_i^w (1 - 5u_i^w u_i^w) \right] \left[\sum_{i=1}^{n} w_i b_i^w (1 - 5v_i^w v_i^w) \right] \right),$$

where now the weights a_i^w and b_i^w are

$$a_i^w = (1 - u_i^w u_i^w) I(1 - |u_i^w|) \quad \text{and} \quad b_i^w = (1 - v_i^w v_i^w) I(1 - |v_i^w|)$$

and

$$u_i^w = \frac{x_i - \mathrm{wmed}(x, w)}{9 \, \mathrm{wmad}(x, w)} \quad \text{and} \quad v_i^w = \frac{y_i - \mathrm{wmed}(y, w)}{9 \, \mathrm{wmad}(y, w)}.$$

The notation wmed denotes the weighted median and wmad denotes the raw weighted median absolute deviation. Let $x_{(1)}, \ldots, x_{(n)}$ denote the order statistics. Since $\sum_{i=1}^{n} w_i = 1$, the weighted median is defined as the element $x_{(k)}$ for which the total weight of all elements $x_{(i)} < x_{(k)}$ is less than or equal to $1/2$ and for which the total weight of all elements $x_{(i)} > x_{(k)}$ is less or equal to $1/2$; see, for example, Cormen, Leiserson and Rivest (1990). The raw weighted median absolute deviation is defined analogously.

The robust exponentially weighted midcorrelation is then defined as

$$(9) \qquad r_{wb} = \frac{s_{wbxy}}{\sqrt{s_{wbxx} s_{wbyy}}}.$$

Like the biweight midcorrelation in (8), the exponentially weighted midcorrelation in (9) effectively suppresses the effects of outliers; however, it also allows us to treat time-varying correlations. Conditions in electricity markets, just like financial markets, can change quite abruptly, and so covariances may be quite unstable and it is better to use estimates that are weighted more heavily on recent hourly data to capture current market conditions. Unlike the exponentially weighted moving correlation is (5), the exponentially weighted midcorrelation in (9) is not guaranteed to produce a positive definite global correlation matrix when the same value of λ is used in the computation of all pairwise correlations. This is not an issue for the application treated herein, but it would be if we wished to carry out optimal portfolio selection in financial markets, for example.

4. Simulation study. Before applying our proposed robust approach to our electricity price returns data, we examine the robustness properties of our robust exponentially weighted midcorrelation and evaluate its performance, and that of other dependence measures detailed in Section 3, in a setting where the true correlation is known.

4.1. *Normal margins.* First, we compare the robustness properties of the robust exponentially weighted midcorrelation in (9) and the Pearson-like exponentially weighted moving correlation in (5). We consider series of length $T = 1000$ of $z_t \sim N(0, \boldsymbol{R}_t)$. Entries on the diagonal of $\boldsymbol{R}_t$ are set to 1, and three different correlation processes are considered for the off-diagonal entries of $\boldsymbol{R}_t$:

a. sine $\rho_t = 0.5 + 0.4 \cos(2\pi t / 200)$
b. fast sine $\rho_t = 0.5 + 0.4 \cos(2\pi t / 20)$
c. ramp $\rho_t = \mathrm{mod}(t / 200)$.

Then we create data with $\gamma\%$ spikes by generating the innovations from a mixture. More precisely, we first consider

$$\begin{bmatrix} z_{t,1} \\ z_{t,2} \end{bmatrix} \sim (1 - \gamma)\% N(0, \boldsymbol{R}_t) + \gamma\% \begin{bmatrix} \delta N(0, 1) + (1 - \delta)\zeta \\ (1 - \delta) N(0, 1) + \delta\zeta \end{bmatrix},$$

where $\delta \sim$ Bernoulli(0.5). These simulated data are normal with marginal outliers. We also simulate data with two different types of bivariate outliers: generating (i) $\gamma\%$ data which are equal to $[\zeta, \zeta]$, or (ii) $\gamma\%$ data which are equal to $[\zeta, -\zeta]$. We call case (i) bivariate positive outliers and case (ii) bivariate negative outliers, as the first should increase nonrobust correlation estimates while the second should decrease them. We consider spikes of three different sizes: $\zeta = 3, 6$ or 9. More precisely, we present results from six scenarios: (1) $\gamma = 0$, (2) $\gamma = 3\%$ and $\zeta = 3$, (3) $\gamma = 3\%$ and $\zeta = 6$, (4) $\gamma = 3\%$ and $\zeta = 9$, (5) $\gamma = 10\%$ and $\zeta = 9$, (6) $\gamma = 20\%$ and $\zeta = 9$. The last scenario is unlikely in our electricity market prices data, but we include it to examine the breakdown properties of our new robust estimator. Results are shown for $\lambda = 0.96$, but are qualitatively the same for neighboring values. The performance of each method is assessed using the root mean square error (RMSE) defined as

$$RMSE = \sqrt{(T - T_0)^{-1} \sum_{t=T_0}^{T} (\hat{\rho}_t - \rho_t)^2}$$

and the mean bias defined as

$$\text{bias} = (T - T_0)^{-1} \sum_{t=T_0}^{T} (\hat{\rho}_t - \rho_t),$$

where $T_0 = 100$ so that exponentially weighted estimates are based on a sufficiently lengthy past. Figures 5 and 6 show results for 200 replications of series of length $T = 1000$ from each of the three correlation models and each of the three contamination models. We see that both estimators perform well when there is no contamination and that the robust estimator is very efficient. The usual Pearson-like exponentially weighted moving correlation breaks down quite quickly for all three correlation processes, the bias increasing considerably with the size and/or amount of contamination. The robust exponentially weighted midcorrelation performs very well. It does not completely recognize and sufficiently downweight the mild 3% contamination where $\zeta = 3$. It suffers some breakdown under 20% contamination with $\zeta = 9$. The exponential weighting nature of the estimator makes it such that if too many point mass outliers of the same value appear in the 100-observation window, then the weighted MAD becomes 0 and the midcorrelation is undefined. While this did not happen at 20% contamination, it does for larger amounts. The size of the bias for the nonrobust estimator is quite considerable and makes this estimator unusable for valid inference when spikes are present.

4.2. *log-GARCH margins.*

Now, we examine models that are more consistent with our electricity market returns data. We consider series of length $T = 1000$ of uncontaminated data $Y_t = \varepsilon_t$, where

$$\ln \sigma_{1,t}^2 = 0.005 + 0.3 \ln \varepsilon_{1,t-1}^2 + 0.6 \ln \sigma_{1,t-1}^2,$$

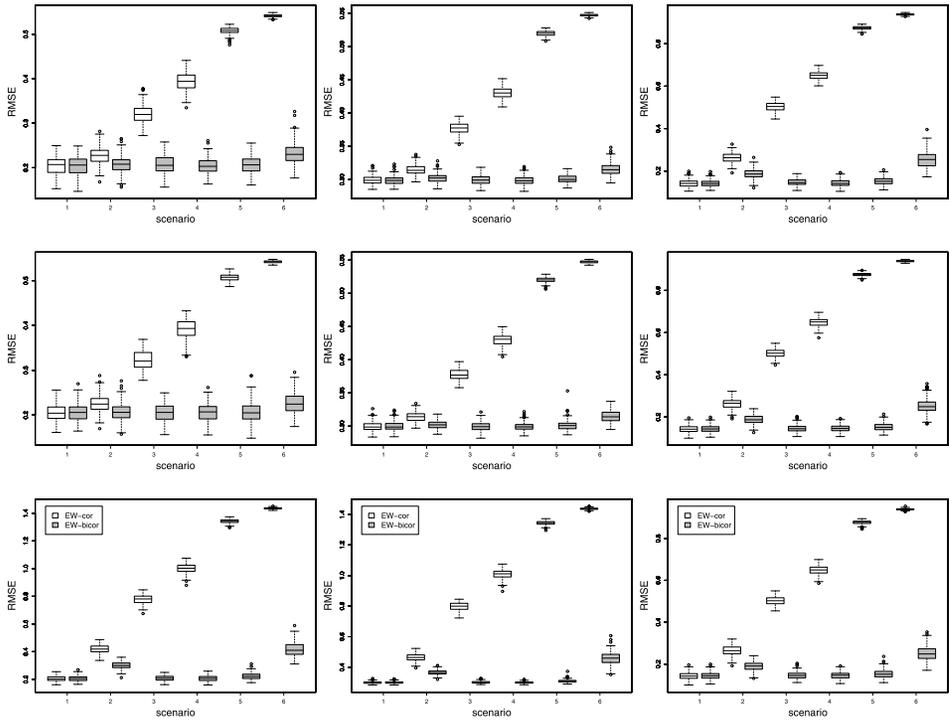$$\ln \sigma_{2,t}^2 = 0.001 + 0.15 \ln \varepsilon_{2,t-1}^2 + 0.8 \ln \sigma_{2,t-1}^2$$

FIG. 5.   *RMSE for* 200 *simulations of series of length* $T = 1000$. *Results are for sine* (*left column*), *fast sine* (*middle column*) *and ramp* (*right column*) *models described in Section* 4.1, *and marginal outliers* (*top row*), *bivariate positive outliers* (*middle row*) *and bivariate negative outliers* (*bottom row*) *for the six scenarios described in Section* 4.1.

and $\varepsilon_t = \sigma_{i,t}z_{t,i}$, $z_{t,i}$ as in Section 4.1. We consider marginal outliers and the first four spike scenarios. We show results for five different approaches. First, we consider the dynamic conditional correlation (DCC) model of Engle (2002) fitted using the two-step DCC estimator described therein. In the last four approaches, the log-GARCH$(1, 1)$ model is fitted in a first step. Then the correlation ρ_t is estimated following (i) the exponentially weighted moving correlation in (5), (ii) the Spearman correlation in (6) calculated using observations at indices $t - 41$ through $t - 1$, (iii) the exponentially weighted Kendall's tau in (7), and (iv) the exponentially weighted midcorrelation in (9). We considered large smoothing constants λ, assuming that volatility in electricity markets is very persistent but not highly reactive as in most equity markets; see, for example, Alexander (2001).

Estimated marginal log-GARCH$(1, 1)$ parameters for 200 replications of series of length $T = 1000$ from the sine correlation model are shown in Figure 7. The log-GARCH$(1, 1)$ model indeed reduces the impact of spikes on marginal volatility parameters and shock, and persistence parameters are unbiasedly estimated even under the largest spikes. Marginal parameter estimates (not shown) for
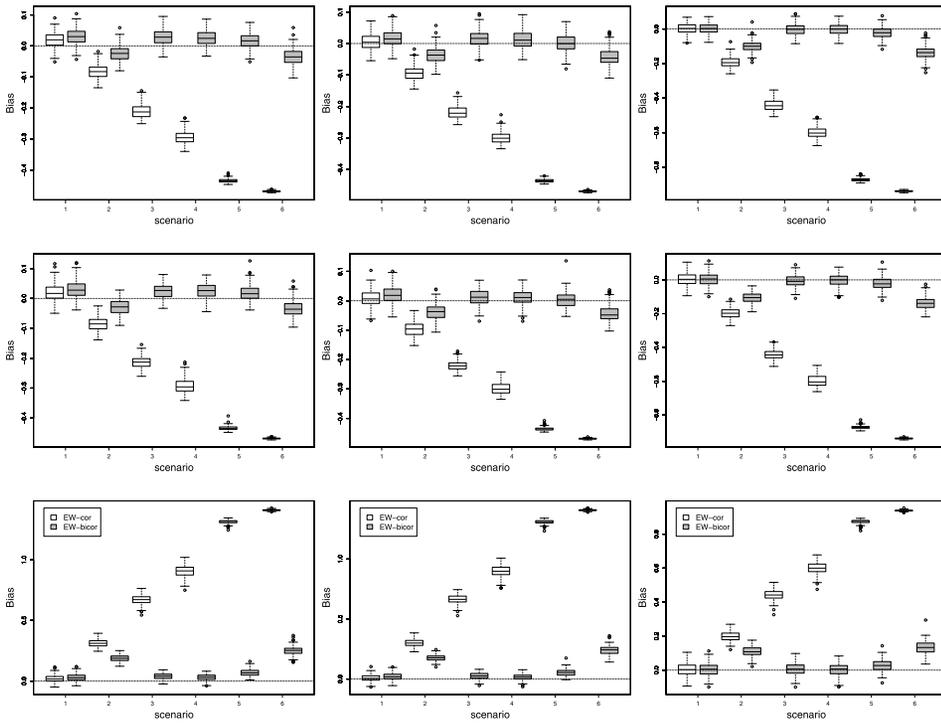
FIG. 6.   *Bias for* 200 *simulations of series of length T* = 1000. *Results are for sine* (*left column*), *fast sine* (*middle column*) *and ramp* (*right column*) *models described in Section* 4.1, *and marginal outliers* (*top row*), *bivariate positive outliers* (*middle row*) *and bivariate negative outliers* (*bottom row*) *for the six scenarios described in Section* 4.1.

the other two correlation models are similar. Performance results for 200 replications of series of length $T = 1000$ from each of the three correlation models appear in Figure 8. We see that both methods that do not have a robust estimator of correlation give very poor estimates of the time-varying correlation for the bulk of the data in the presence of spikes, and the performance gets worse with the size of the spikes. In the case of a slowly-varying sine correlation, a Spearman correlation based on the last 40 observations works surprisingly well. Results are almost as good as those of the robust exponentially weighted midcorrelation and only slightly more variable. The benefits of the exponential weighting in the midcorrelation are clearer on the rapid-varying fast sine and ramp correlations. The exponentially weighted Kendall's tau offers the best performance among robust estimators for the ramp correlation model, but is the worst robust performer in both sine correlation models. Overall, robust exponentially weighted midcorrelation offers the best performance of all methods. As with all robust estimators, there is some loss of efficiency in the case of no contamination.
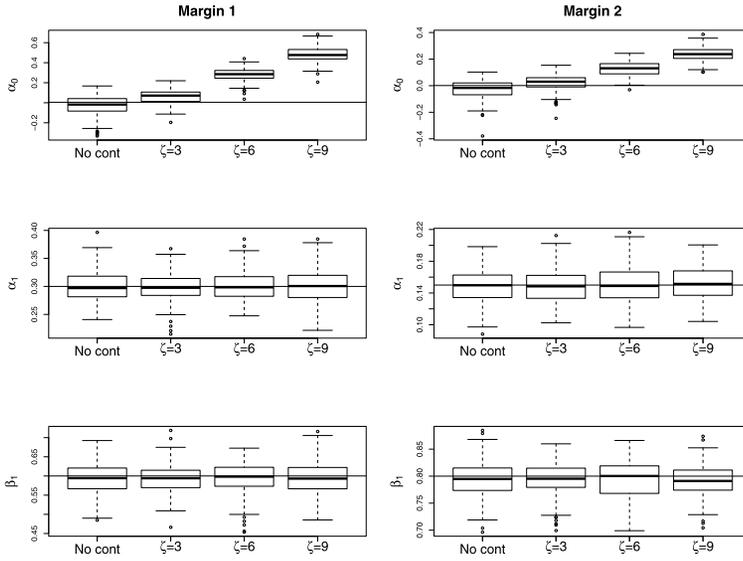
FIG. 7.   *Estimated marginal* log-GARCH(1, 1) *parameters for* 200 *simulations of series of length*
T = 1000 *for the sine model described in Section* 4. *Results are for uncontaminated data and* 3%
spike innovations of size 3, 6 *and* 9, *respectively, in each panel. The horizontal line indicates the true*
value of the parameter.

5. Electricity price returns.   We consider the log return at hour *t* for each of
the 15 NYCA zones over the 1 January 2009 to 31 December 2014 period. Data
for February 29 are removed.

5.1. *Marginal models.*   The key drivers for the day-ahead load forecasting
models of the NYISO are day-type and weather [New York Independent System
Operator (2013)], and these variables are also likely to be important regressors
in the marginal mean and variance models for the log return. For the marginal
mean model, the matrix $\boldsymbol{D}_{h(t)}$ of dummy variables includes six binary variables
for day of the week, a binary variable for public holidays, and day of year har-
monics up to order 3.[8] The matrix $\boldsymbol{X}_{h(t)}$ contains an hourly temperature variable
and two dummy variables to pick up extreme temperatures in the bottom and top
0.5% for the zone, respectively. Following New York Independent System Opera-
tor (2013), we aggregate weather from 17 stations across New York into 11 zone
points based on population and other historical weighting factors. Weather sta-
tion weights imputed to each of the 11 internal zones are as in Table B-3 of New
York Independent System Operator (2013). For each of the four external zones, we
choose a weather station in close proximity to the external connection. Weather
stations used for each zone are shown in Figure 9. We use the hourly temperature

---

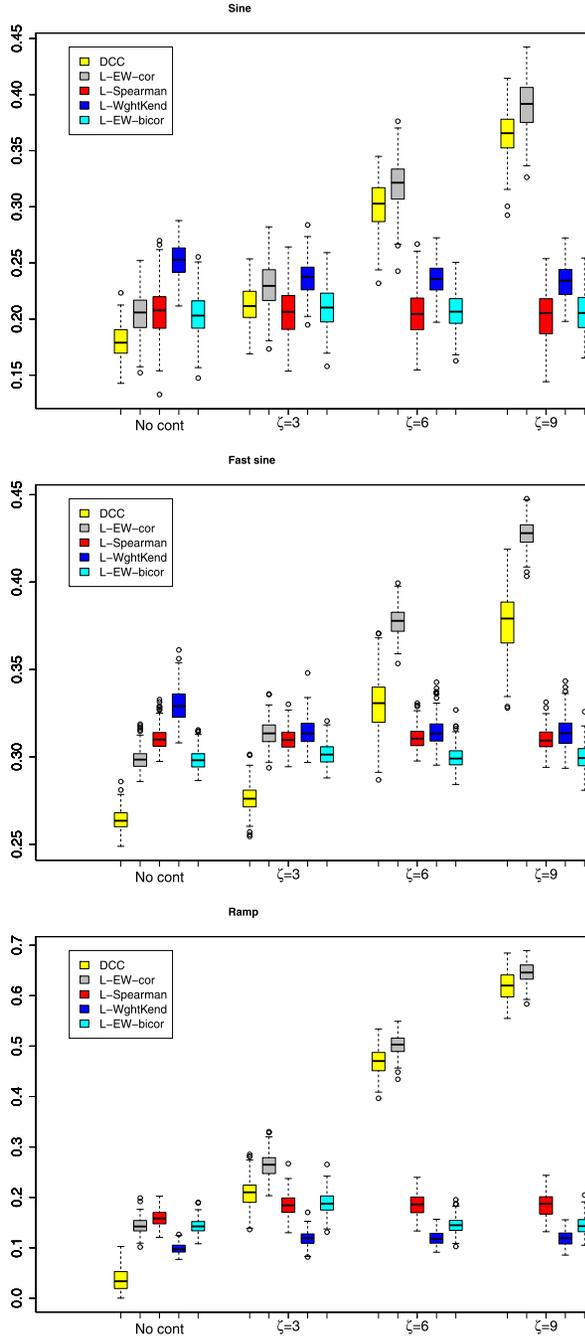[8]Terms in $\cos(2\pi kt/365)$ and $\sin(2\pi kt/365)$ for $k = 1, 2, 3$.

FIG. 8. *RMSE for* 200 *simulations of series of length T* = 1000. *Results for the sine* (*top panel*), *fast sine* (*middle panel*) *and ramp* (*bottom panel*) *models described in Section* 4. *Results are for un-contaminated data and* 3% *spike innovations of size* 3, 6 *and* 9, *respectively, in each panel. Results shown for smoothing values* λ = 0.96 (*EW-cor and EW-bicor*) *and, equivalently,* α = 0.04 (*WghtK-end*).
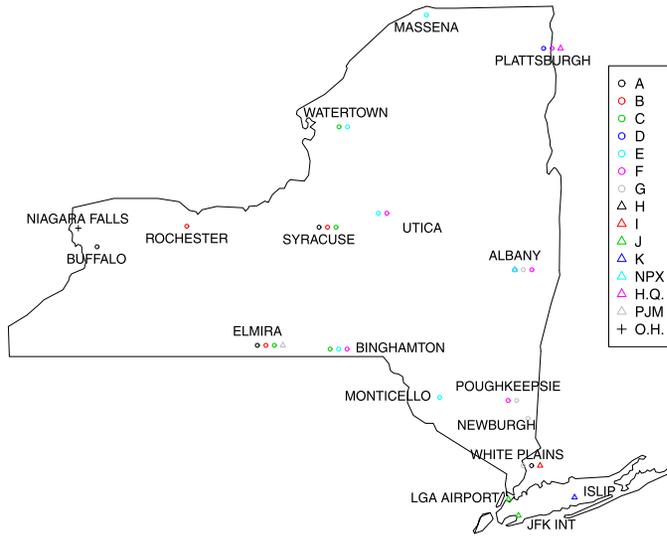
FIG. 9. *Weather stations imputed to each zone to establish the temperature value for the zone. Weights imputed to each of the* 11 *internal zones as in Table B-*3 *of NYISO* (2013).

as our weather variable. The temperature data are recorded to the nearest tenth of a degree Celsius and are obtained from the National Oceanic and Atmospheric Administration (NOAA) at www.nesdis.noaa.gov. These series have very few missing observations, and we simply filled in missing points by linear interpolation. For the marginal variance model, the matrix $D_{h(t)}$ only includes the day of week and public holiday binary variables. The matrix $X_{h(t)}$ contains an hourly temperature variable, a natural gas price variable,[9] a leverage term and volatility proxies for the other 14 zones. Parameters in equations (1)–(4) are estimated as described in Section 2.2. For the mean model, the values $P = 1$ and $p = 2$ are found to be sufficient, and are used for all zones. No attempt is made to find optimal values for each of the zones. For the variance model, explanatory variables were added to the model one at a time to favor convergence. We retained a final model based on the BIC criterion for models that passed the Li and Mak (1994) test.[10]

Table 1 shows the skewness and excess kurtosis of residuals from the second least median of squares fit and the log-GARCH(1, 1)-X models, respectively, for the 15 zones. As expected, there are electricity price spikes.

---

[9]There is a high level of dependence between natural gas and electricity prices in the state of New York; see, e.g., Pineau, Dupuis and Cenesizoglu (2015). We use the Henry Hub Natural Gas Spot Price in dollars per MMBtu, available from EIA (2015). Economic activity and population is considered fixed over the short six-year period.

[10]In a few cases, no log-GARCH-X model devolatilized the series sufficiently well to pass the Li and Mak (1994) test. In those cases, the retained model was based on BIC alone.

TABLE 1
Summary statistics of residuals of mean and variance models. Skewness and excess kurtosis of residuals of mean and variance models fitted to data for each NYCA zone

Zone	Mean model		Variance model	
	Skewness	Kurtosis	Skewness	Kurtosis
A	0.25	16	−0.90	76
B	−0.93	43	1.2	114
C	−0.12	21	−0.49	84
D	0.00	64	−0.09	99
E	−0.02	19	0.26	60
F	0.06	11	0.59	21
G	0.11	9.6	−0.07	42
H	−0.04	10	0.09	62
I	−0.11	10	0.62	56
J	−0.01	7.9	−0.70	32
K	−0.11	10	−0.11	12
NPX	0.09	17	−0.18	29
H.Q.	−0.13	472	−2.4	188
PJM	0.11	11	0.01	16
O.H.	0.30	20	0.21	30

Figure 10 shows the estimated value of the GARCH persistence parameter β_1 in the log-GARCH(1, 1)-X model for each hour and each zone. The persistence is small with the exception of zones N.Y.C, LONGIL, H.Q. and PJM. N.Y.C. is the most populated zone [42.1% of the state population, New York Independent System Operator (2013)], and it consumed the largest proportion (33%) of electricity among NYCA zones over the 2009–2014 period of our study. Its dominating size explains the larger levels of persistence. Long Island is the least interconnected zone within the NYCA. Networking problems make it such that the zone must sometimes depend on its own thermal power plants to meet demand within the zone. This leads to price changes that are not necessarily shared with other zones. H.Q. and PJM are external zones which must additionally deal with issues outside of NY state, and this explains their larger levels of persistence. Estimated leverage parameters are sometimes significant, but not always. When significant, they are negative or positive with no particular tendency (results not shown). Spillover terms in the log-GARCH-X models can make a strong contribution to the time-varying volatility. Figure 11 shows ratios of the estimated value of spillover parameters to their estimated standard error when volatility proxies are retained in the hourly log-GARCH(1, 1)-X model. For a given zone, there is greater spillover from directly connected zones. Zones that showed larger volatility persistence in Figure 10 are less affected by spillover volatility.
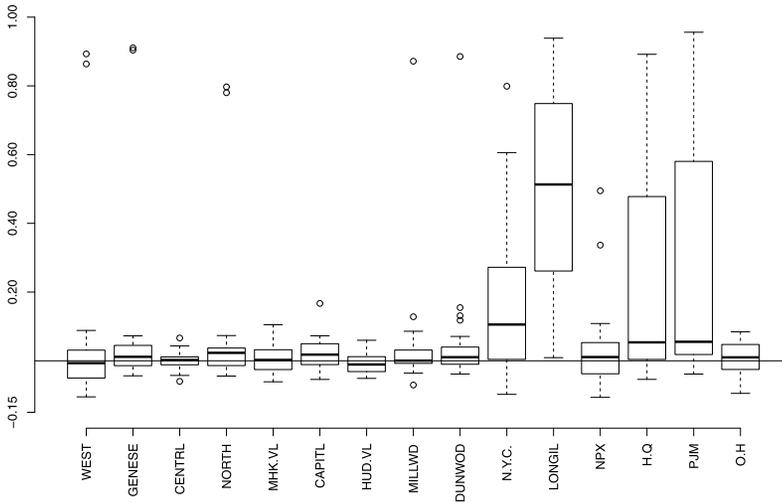
FIG. 10.   *Estimated value of the persistence parameter β_1 in the hourly* log-GARCH(1, 1)-*X model.*

5.2. *Zone correlations.*   The correlation between the detrended-devolatilized log returns for NYCA zones is estimated robustly using the exponentially weighted midcorrelation in (9). Residuals from the fitted model (4) are used as a proxy for the detrended-devolatilized log return for each zone.

Robustly estimated correlations with N.Y.C. and H.Q. are shown in Figure 12. Several interesting points emerge for correlation values with N.Y.C. (left panel):
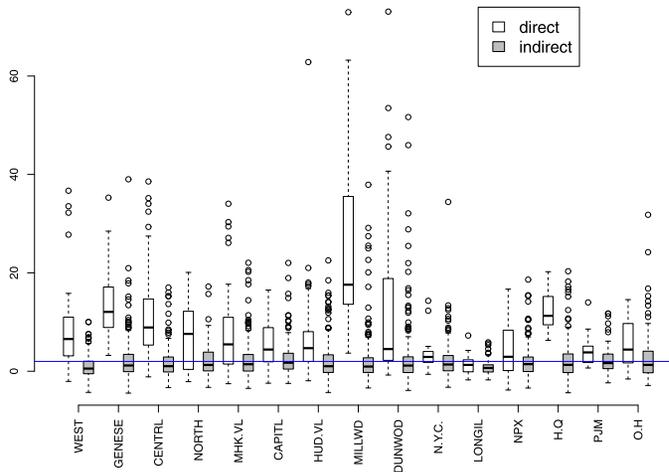
FIG. 11.   *Ratio of the estimated value of spillover parameters to their estimated standard error for zones with a direct connection* (*direct*) *and indirect connection* (*indirect*) *when volatility proxies are retained in the hourly* log-GARCH(1, 1)-*X model.*
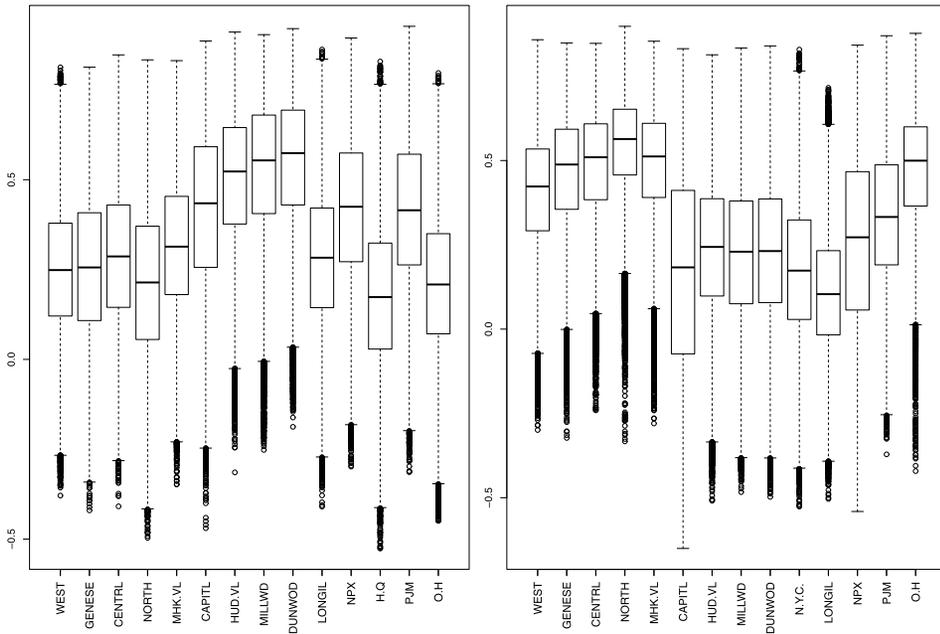
FIG. 12.   *Robustly estimated correlations between the detrended-devolatilized hourly log returns in zone N.Y.C. and other zones (left) and in zone H.Q. and other zones (right). Based on data over the 1 January 2009 to 31 December 2014 period.*

(i) they are not in the same range for every zone pair, (ii) they are mostly positive, but can be negative, (iii) they are the highest with neighboring zones to the north (G, H and I), and (iv) they are weaker with immediate neighbor Long Island (K). The weaker interconnectedness of Long Island detailed earlier explains (iv). With H.Q. (right panel), we note the following: (i) greater values with neighboring zones D and O.H., (ii) slightly smaller correlation overall than between N.Y.C. and other zones. As the only NYCA connection to a regulated market,[11] the H.Q. zone does not follow the rules of a competitive market, and its price changes may not reflect those of other NYCA zones.

5.3. *Partial correlations.*   There are 23 transmission service areas contained within the 15 NYCA zones. They are shown as edges in Figure 13 and may represent multiple transmission facilities. As there can be multiple paths between any two zones, it is difficult to interpret the correlation estimate between two zones. To isolate the dependence between a zone and one of its directly connected neighbors, we look at the partial correlation between the price changes in the two zones. Partial correlation measures the degree of association between two random variables, after having removed the effect of a set of controlling random variables.

---

[11]Hydro-Quebec is a government-owned public utility.

More technically, the partial correlation between X and Y given a set of n controlling variables $\mathbf{Z} = \{Z_1, Z_2, \ldots, Z_n\}$, written $r_{XY \cdot \mathbf{Z}}$, is the correlation between the residuals resulting from the linear regression of X with $\mathbf{Z}$ and of Y with $\mathbf{Z}$, respectively. The nth-order partial correlation (i.e., with $|\mathbf{Z}| = n$) can be easily computed from three $(n - 1)$th-order partial correlations. The zeroth-order partial correlation $r_{XY \cdot \varnothing}$ is defined to be the regular correlation coefficient r_{XY}. For any $Z_0 \in \mathbf{Z}$, we have

$$(10) \qquad r_{XY \cdot \mathbf{Z}} = \frac{r_{XY \cdot \mathbf{Z} \setminus \{Z_0\}} - r_{XZ_0 \cdot \mathbf{Z} \setminus \{Z_0\}} r_{Z_0 Y \cdot \mathbf{Z} \setminus \{Z_0\}}}{\sqrt{1 - r_{XZ_0 \cdot \mathbf{Z} \setminus \{Z_0\}}^2} \sqrt{1 - r_{Z_0 Y \cdot \mathbf{Z} \setminus \{Z_0\}}^2}};$$

see, for example, Kendall and Stuart (1979). We compute robust partial correlation estimates by applying (10) recursively, using our robust exponentially weighted midcorrelations computed as in (9) as the zeroth-order partial correlation coefficient. These robust partial correlations are plotted in Figure 13 for directly connected neighbors to each zone. It is clear that all transmission service areas are not created equally and do not allow for their connecting zones to benefit/suffer from price changes equally. For some, the distribution of the partial correlation is roughly symmetric about 0. Some internal zones are more in sync with their directly connected external zone than with their directly connected internal zone; see, for example, zone F with NPX. Nothing in the price-setting protocol [New York Independent System Operator (2013)] would lead us to believe that this is the case.

Available transfer capability (ATC) data are also available at www.nyiso.com for some of the transmission service areas. In Figure 14, ATC at six internal interfaces are shown along with the partial correlations for the zones they connect. The percentage of NYCA electricity consumed by the latter zones is also indicated. It is clear that the dependencies are not a function of ATC and consumption only. For example, the Dysinger East transmission service area (i) has roughly half the ATC of the UPNY/CONED transmission service area, (ii) connects two zones that consume double that of the zones connected by UPNY/CONED, and yet (iii) results in partial correlations quite comparable to those produced for the zones connected by UPNY/CONED. On the other hand, the small ATC for transmission service area CENT EAST could explain the small, and even often negative, partial correlations between zones E and F.

Robustly estimated partial correlations in Figures 13 and 14 are over the 1 January 2009 to 31 December 2014 period. It is interesting to regress these correlations on potential explanatory variables and identify possible significant differences in the correlations across different levels of the factors. To establish the significance of the effects, the Newey and West (1987) procedure is used to adjust the covariance matrix of the parameters to account for autocorrelation and heteroskedasticity. While the explanatory variables listed in Section 5.1 could explain in part the level of partial correlation between detrended-devolatilized log returns
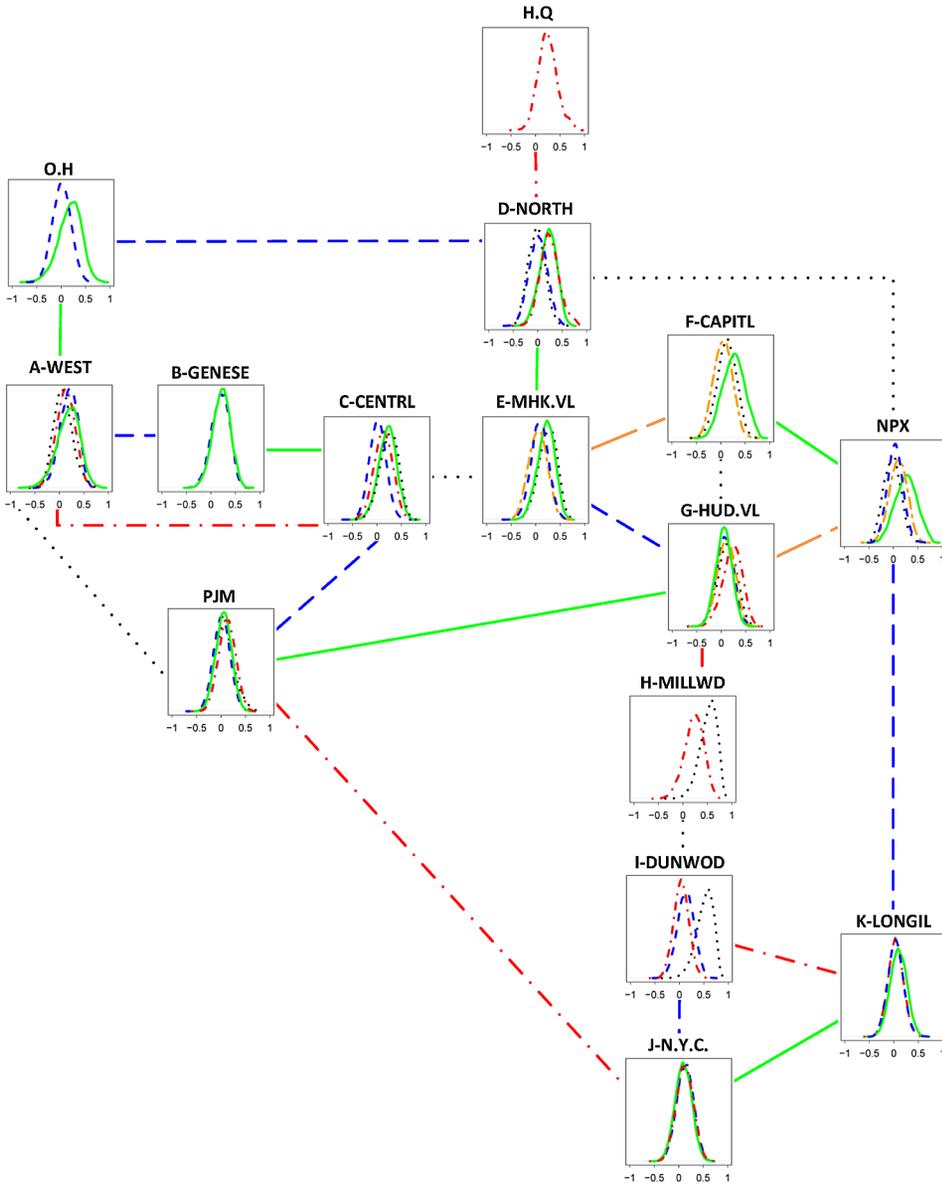
FIG. 13.   *NYISO zones and transmission service areas (shown as lines of different types) connecting them. For each zone, the robustly estimated partial correlation between its detrended-devolatilized hourly log returns and those of directly connected zones is shown. For a given zone, the kernel density estimate curve is the same color/type as the line representing the transmission service area to which it corresponds. Based on data over the* 1 *January* 2009 *to* 31 *December* 2014 *period.*
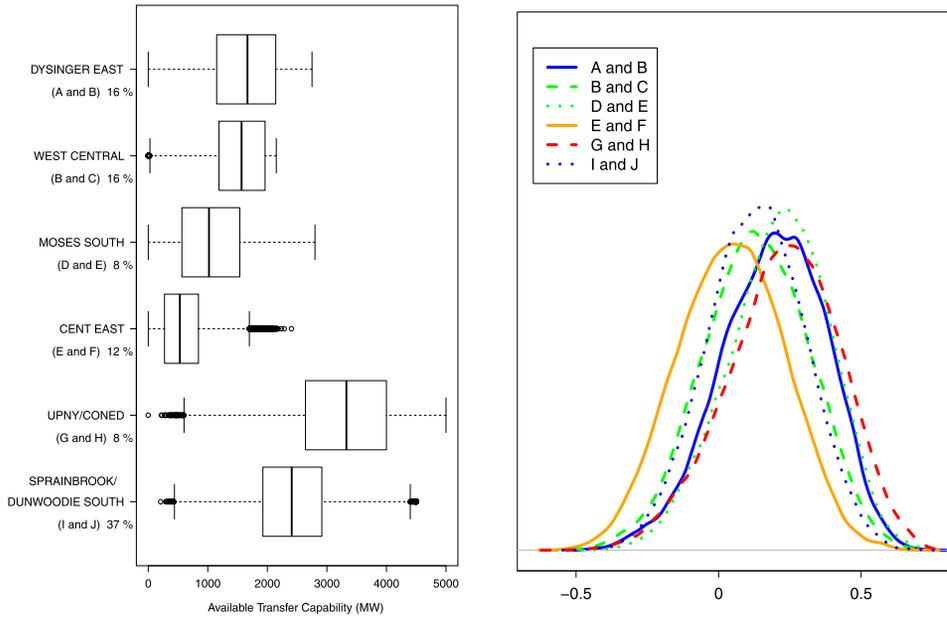
FIG. 14.   *Left plot*: *Available transfer capability at six internal interfaces* (*connected zones in parentheses*). *The percentage of NYCA electricity use for zones also appears. Right plot*: *Robustly estimated partial correlation between the detrended-devolatilized hourly log returns for connected zones. Based on data over the* 1 *January* 2009 *to* 31 *December* 2014 *period*.

from two directly connected zones, congestion due to planned outages or accidental network breaks could also have an effect. As complete data on congestion due to outages and accidental network breaks are not available, we follow Ben Amor et al. (2014) and use the absolute difference in price levels between the two zones as a proxy. Ben Amor et al. (2014) use a \$5 threshold as an indicator of congestion. We create a congestion factor variable by dividing according to price differential (D in \$) into four levels: $[0, 5)$, $[5, 10)$, $[10, 15)$ and $[15, \infty)$. We also take a factor approach to isolating the impact of hourly temperature and natural gas prices.[12] While some effects are significant (results not shown), the size of most effects remains quite small and of no practical significance; plots of partial correlations for different levels of the factors remain essentially as in Figure 13. One notable exception is the effect of congestion for some zonal pairs. In Figure 15, such pairs are shown. The effects are as anticipated, with increased absolute price differential leading to less correlation in the price changes.

Finally, in the case of an electricity grid, *spatial* proximity is better described by the number of intermediary zones between two given zones. Transmission service

---

[12]We divide temperatures (in $^{\circ}C$) into five levels: $(-\infty, 0]$, $[0, 16)$, $[16, 20)$, $[20, 28)$ and $[28, \infty)$. We divide natural gas prices (in \$) into three levels: $[0, 3)$, $[3, 5)$ and $[5, \infty)$.
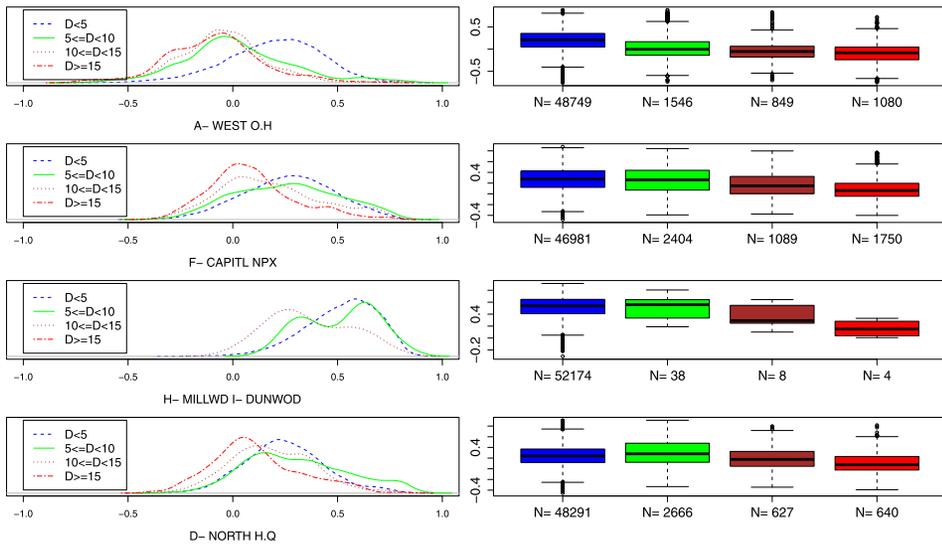
FIG. 15. *Robustly estimated partial correlation between the detrended-devolatilized hourly log returns for connected zones under different absolute price differences. The number of observations N for the level of the factor is shown below the boxplot. Based on data over the* 1 *January* 2009 *to* 31 *December* 2014 *period.*

areas between zones are shown in Figure 13. We found the number of intermediaries to be a poor predictor of partial correlations (results not shown). Returns in some zones have very poor partial correlation with returns in their connected zones (see Figure 13), and the partial correlation is no poorer for zones many intermediaries away.

6. Discussion. As part of its mission, the NYISO must provide factual information to policymakers, stakeholders and investors in the power system. The analyses herein seek to move from the raw LBMP hourly zonal price data made available to an understanding of market price dynamics within the system. Our proposed methodology enables the computation of robust detrended-devolatilized price-change correlation estimates for any two zones within the NYCA and shows that these correlations can vary considerably by pair. To isolate the dependence between a zone and one of its directly connected neighbors, we look at partial correlation between the price changes in the two zones. We see that in terms of price-change dynamics, the zones are not as *connected* as an equitable statewide market would wish; even adjacent zones with transmission service areas showing large available transmission capability may not have large price-change correlations. Our analysis is the first to provide such an assessment. The methodology presented herein can be applied to any electricity market.

Regression analyses were performed in an attempt to explain the time-varying partial correlations for a given pair of zones, and many regressors were included.

Only price differential was found to be practically significant, and this for only four pairs. As for any differences between the partial correlations of different pairs, they could not be easily explained. Investigating the relationships between our estimated partial correlations and the characteristics of the underlying network grid could provide additional information for investment. Such an analysis requires access to, and understanding of, much technical data and is out of the scope of this paper.

REFERENCES

ALEXANDER, C. (2001). *Market Models*. Wiley, Chichester.

BEN AMOR, M., BILLETTE DE VILLEMEUR, E., PELLAT, M. and PINEAU, P.-O. (2014). Influence of wind power on hourly electricity prices and GHG (greenhouse gas) emissions: Evidence that congestion matters from Ontario zonal data. *Energy* **66** 458–469.

CHRISTENSEN, T. M., HURN, A. S. and LINDSAY, K. A. (2012). Forecasting spikes in electricity prices. *International Journal of Forecasting* **28** 400–411.

CORMEN, T. H., LEISERSON, C. E. and RIVEST, R. L. (1990). *Introduction to Algorithms*. MIT Press, Cambridge, MA. MR1066870

EIA (2015). *Henry Hub Natural Gas Spot Price*. US Energy Information Administration, Washington. Web site accessed on January 15, 2015. http://www.eia.gov/dnav/ng/hist/rngwhhdd.htm.

ENGLE, R. (2002). Dynamic conditional correlation: A simple class of multivariate generalized autoregressive conditional heteroskedasticity models. *J. Bus. Econom. Statist.* **20** 339–350. MR1939905

EYDELAND, A. and WOLYNIEC, K. (2012). *Energy and Power Risk Management*, 2nd ed. Wiley, Hoboken, NJ.

FISHER, T. J. and GALLAGHER, C. M. (2012). WeightedPortTest: Weighted portmanteau tests for time series goodness-of-fit. R package version 1.0. Available at https://CRAN.R-project.org/package=WeightedPortTest.

FRANCQ, C. and SUCARRAT, G. (2017). An equation-by-equation estimator of a multivariate log-GARCH-X model of financial returns. *J. Multivariate Anal.* **153** 16–32. MR3578836

GEMAN, H. and RONCORNI, A. (2006). Understanding the fine structure of electricity prices. *Journal of Business* **79** 1225–1261.

HELLSTRÖM, J., LUNDGREN, J. and YU, H. (2012). Why do electricity prices jump? Empirical evidence from the nordic electricity market. *Energy Economics* **34** 1774–1781.

HICKEY, E., LOOMIS, D. G. and MOHAMMADI, H. (2012). Forecasting hourly electricity prices using ARMAX-GARCH models: An application to MISO hubs. *Energy Economics* **34** 307–315.

JANCZURA, J., TRÜCK, S., WERON, R. and WOLFF, R. C. (2013). Identifying spikes and seasonal components in electricity spot price data: A guide to robust modeling. *Energy Economics* **38** 96–110.

KARAKATSANI, N. V. and BUNN, D. W. (2008). Forecasting electricity prices: The impact of fundamentals and time-varying coefficients. *International Journal of Forecasting* **24** 764–785.

KENDALL, M. G. and STUART, A. (1979). *The Advanced Theory of Statistics, Vol. 2. Inference and Relationship*. London, Griffin.

LANGFELDER, P. and HORVATH, S. (2008). WGCNA: An R package for weighted correlation network analysis. *BMC Bioinformatics*.

LANGFELDER, P. and HORVATH, S. (2012). Fast R functions for robust correlations and hierarchical clustering. *J. Stat. Softw.* **46** 1–17.

LAX, D. A. (1985). Robust estimators of scale: Finite-sample performance in long-tailed symmetric distributions. *J. Amer. Statist. Assoc.* **80** 736–741.

LI, W. K. and MAK, T. K. (1994). On the squared residual autocorrelations in nonlinear time series with conditional heteroskedasticity. *J. Time Series Anal.* **15** 627–636. MR1312326

NEW YORK INDEPENDENT SYSTEM OPERATOR (2013). Day-Ahead Scheduling Manual. Schenectady, New York.

NEW YORK INDEPENDENT SYSTEM OPERATOR (2014). Power Trends 2014: Evolution of the Grid. Schenectady, New York.

NEWEY, W. K. and WEST, K. D. (1987). A simple, positive semidefinite, heteroskedasticity and autocorrelation consistent covariance matrix. *Econometrica* **55** 703–708. MR0890864

NOWOTARSKI, J., TOMCZYK, J. and WERON, R. (2013). Robust estimation and forecasting of the long-term seasonal component of electricity spot prices. *Energy Economics* **39** 13–27.

PÊNA, J. I. (2012). A note on panel hourly electricity prices. *Journal of Energy Markets* **5** 81–97.

PINEAU, P.-O., DUPUIS, D. J. and CENESIZOGLU, T. (2015). Assessing the value of power interconnections under climate and natural gas price risks. *Energy* **82** 128–137.

POZZI, F., DI MATTEO, T. and ASTE, T. (2012). Exponential smoothing weighted correlations. *Eur. Phys. J. B* **85** 175.

SHOEMAKER, L. H. and HETTMANSPERGER, T. P. (1982). Robust estimates and tests for the one- and two-sample scale models. *Biometrika* **69** 47–53. MR0655669

SUCARRAT, G. (2014). lgarch: Simulation and estimation of log-GARCH models. R package version 0.5. Available at http://CRAN.R-project.org/package=lgarch.

SUCARRAT, G. and ESCRIBANO, Á. (2014). Unbiased Estimation of Log-GARCH Models in the Presence of Zero Return. MPRA Paper 59040.

SUCARRAT, G., GRØNNEBERG, S. and ESCRIBANO, A. (2016). Estimation and inference in univariate and multivariate log-GARCH-X models when the conditional density is unknown. *Comput. Statist. Data Anal.* **100** 582–594.

WILCOX, R. R. (2012). *Introduction to Robust Estimation and Hypothesis Testing*, 3rd ed. Academic Press, San Diego, CA.

DEPARTMENT OF DECISION SCIENCES
HEC MONTRÉAL
3000 CHEMIN DE LA CÔTE-SAINTE-CATHERINE
MONTRÉAL (QUÉBEC), H3T 2A7
CANADA
E-MAIL: debbie.dupuis@hec.ca